PTHrP Regulates Angiogenesis and Bone Resorption *via* VEGF Expression

SACHIKO ISOWA[1], TSUYOSHI SHIMO[1], SOICHIRO IBARAGI[1], NAITO KURIO[1], TATSUO OKUI[1], KIMINORI MATSUBARA[2], NUR MOHAMMAD MONSUR HASSAN[1] , KOJI KISHIMOTO[1] and AKIRA SASAKI[1]

[1]*Department of Oral and Maxillofacial Surgery, Okayama University Graduate School of Medicine, Dentistry, and Pharmaceutical Sciences, Okayama, Japan;*
[2]*Department of Human Life Science Education, Graduate School of Education, Hiroshima University, Hiroshima, Japan*

Abstract. *Background: Parathyroid hormone-related protein (PTHrP) is a key regulator of osteolytic metastasis of breast cancer (BC) cells, but its targets and mechanisms of action are not fully understood. This study investigated whether/how PTHrP (1-34) signaling regulates expression of vascular endothelial growth factor (VEGF) produced by BC cells. Materials and Methods: A mouse model of bone metastasis was prepared by inoculating mice with tumour cell suspensions of the human BC cell line MDA-MB-231 via the left cardiac ventricle. VEGF expression was examined by Western blot and real-time RT-PCR analysis, as well as by confocal microscopy in the bone microenvironment. Results: PTHrP was expressed in cancer cells producing PTH/PTHrP receptor and VEGF that had invaded the bone marrow, and PTHrP was up-regulated VEGF in MDA-MB-231 in vitro. The culture medium conditioned by PTHrP-treated MDA-MB-231 cells stimulated angiogenesis and osteoclastogenesis compared with control medium, giving a response that was inhibited by VEGF-neutralizing antibody treatment. Inhibition of protein kinase C (PKC) prevented PTHrP-induced extracellular signal-regulated kinase (ERK1/2) and p38 activation, and PTHrP-induced VEGF expression. Conclusion: PTHrP plays an important role in modulating the angiogenic and bone osteolytic actions of VEGF through PKC-dependent activation of an ERK1/2 and p38 signaling pathway during bone metastasis by breast cancer cells.*

Correspondence to: Dr Tsuyoshi Shimo, Department of Oral and Maxillofacial Surgery, Okayama University Graduate School of Medicine, Dentistry and Pharmaceutical Sciences, 2-5-1 Shikata-cho, Okayama, 700-8525, Japan, Tel: +81 (086)2356702, Fax: +81 (086)2356704, e-mail: shimotsu@md.okayama-u.ac.jp

Key Words: PTHrP, parathyroid hormone-related protein, VEGF, vascular endothelial growth factor, angiogenesis, bone resorption, MAPK, mitogen-activated protein kinase.

Bone is one of the most common sites of metastasis for certain types of tumours, especially prostate, breast, and lung carcinomas. After tumour cells find their way to the bone marrow, there are numerous cell types present in the bone microenvironment that are involved in the maintenance of immune and inflammatory responses and whose activity may be modulated by the cytokines and/or growth factors secreted by the tumour cells (1). The progression of osteolytic bone metastasis requires the establishment of functional interactions between metastatic cancer cells and bone cells, and these interactions are mediated by soluble regulators of osteoclast formation, activity, and survival (2).

The expression of parathyroid hormone-related protein (PTHrP) in breast cancer has been associated with increased malignancy (3). It has been proposed that tumour-derived PTHrP plays a critical role in skeletal metastasis by a vicious cycle in which PTHrP enhances bone remodeling and the release of numerous biological factors, thus providing a fertile environment for further tumour growth (4). Tumour-derived PTHrP may also facilitate progression of skeletal metastasis by directly stimulating tumour cell proliferation, adhesion, and survival *via* autocrine or paracrine mechanisms (5-7). Neutralising antibodies against PTHrP are known to inhibit the development and progression of bone metastasis of human breast cancer cells in a mouse model (8).

Vascular endothelial growth factor (VEGF) is the most important essential mediator of angiogenesis (9). Binding of VEGF stimulates endothelial cells to degrade extracellular matrix, to migrate, and to form tubes through its interaction with 2 main membrane-bound cell receptors, *i.e.* KDR/Flk-1 and/or Flt-1 (10). Besides stimulating angiogenesis, VEGF has also been demonstrated to be involved in early haematopoietic development and chemotaxis of monocytes (11, 12). An immunohistological study revealed the expression of VEGF receptors on chondroclasts as well as on endothelial cells (13). In addition, it has recently been demonstrated that VEGF

induces osteoclast formation in conjunction with receptor activator of nuclear factor kappa B (NF-κB) ligand (RANKL) (14). VEGF directly enhances osteoclastic bone resorption through KDR/Flk-1 and/or Flt-1 receptors expressed in mature osteoclasts (15) and VEGF enhancement of osteoclast survival involves β3 integrin-mediated attachment of osteoclasts to the extracellular matrix (16). These findings suggest that VEGF may regulate osteoclast differentiation, activation, and survival as well as angiogenesis.

PTHrP stimulates *VEGF* gene expression in a rapid and transient fashion in osteoblasts (17-19) and in epithelial cells of normal rat renal tubules (20). Because PTHrP is an osteolytic factor closely associated with the induction of neovasculature in bone, and is also involved in osteoclastogenesis, it has been suggested that PTHrP may be functionally related to the biological action of VEGF. However, a possible relationship between PTHrP and VEGF in cancer bone metastasis has not yet been examined. In this study, evidence was obtained for the critical involvement of VEGF in osteolytic metastasis of breast cancer cells and the utility of this factor as a potential new molecular target. Using *in vivo* and *in vitro* models, it was demonstrated that (i) VEGF up-regulation by PTHrP in cancer cells resulted in enhanced proliferation and migration of endothelial cells and osteoclastic bone resorption; and (ii) *VEGF* gene expression was stimulated by PTHrP, and this stimulation was mediated *via* PKA and PKC-dependent activation of an ERK1/2 and p38 pathway.

Materials and Methods

Materials. The following materials were purchased from their respective sources: Human PTHrP-(1-34), dibutyryl-cAMP (db-cAMP), and 12-*O*-tetradecanoylphorbol-13-acetate (TPA), from Sigma (St. Louis, MO, USA); PD98059, SB203580, H89, and GF109203X, from Calbiochem (La Jolla, CA, USA); anti-ERK1/2, pERK1/2, and p38 antibodies, and siRNAs against hp38 (sc-29433), hERK1 (sc-44205), hERK2 (sc-35335), hPKC (sc-29449) and control siRNAs (sc-37007) from Santa Cruz Biotechnology (Santa Cruz, CA, USA); anti-p-p38, from Cell Signaling (Beverly, MA, USA); human anti-VEGF neutralising antibody and recombinant human VEGF, from R&D Systems (Minneapolis, MN, USA). Humanized anti-PTHrP neutralizing antibody (8, 21) was kindly provided by Chugai Research Laboratories (Kanagawa, Japan). TH human VEGF promoter luciferase construct (–850 bp to +1036 bp) was kindly provided by Dr Daniel Chung (Gastrointestinal Unit, Department of Medicine, Massachusetts General Hospital and Harvard Medical School, USA) (22).

Cell line and cell culture. A highly metastatic variant of MDA-MB-231 (23, 24) was cultured in Dulbecco's modified Eagle's medium (DMEM; Invitrogen Corporation, Grand Island, NY, USA) containing 10% foetal calf serum (FCS; JRH Bioscience, Lenexa, KS, USA) and 1% penicillin/streptomycin (Invitrogen Corporation), at 37˚C under an atmosphere of 5% CO_2/air. Normal human umbilical vein endothelial cells (HUVECs) were cultured in endothelial cell growth medium-2 (Cambrex BioScience, Verviers, Belgium). $CD11b^+$ bone marrow cells were cultured in αMEM (modified minimum essential medium; Sigma) with 10% FCS (Hyclone Laboratories, Logan, UT, USA).

Purification of osteoclast progenitors. Bone marrow cells were washed twice by centrifugation in 20 ml of cold buffer containing sterile PBS supplemented with 0.5% bovine serum albumin (BSA; Sigma) and 2 mM EDTA (Sigma). The cell pellet was resuspended in 80 μl buffer per 10^7 cells, and the cells were magnetically labeled by adding 20 μl of anti-CD11b microbeads per 10^7 cells. The cells were next incubated for 30 min on ice and then washed by centrifugation with a volume of buffer 10- to 20-fold that of the labeling volume and resuspended in 500 μl of buffer per 10^8 cells. $CD11b^+$ cells were depleted using an MD depletion column (Miltenyi Biotec Inc Bergisch Gladbach, Germany) placed in the magnetic field of a MidiMACS separation unit (Miltenyi Biotec Inc). On day 7, the cultures were fixed with 60% acetone in citrate buffer (Sigma) and stained for tartrate-resistant acid phosphatase (TRAP) as a marker for osteoclasts by using a Leukocyte Acid Phosphatase Kit (Sigma). Stained TRAP-positive multinucleate cells (3 or more nuclei) were counted manually under a light microscope.

Mouse model of bone metastasis. A mouse model of bone metastasis was prepared by inoculating mice with tumour cell suspensions of MDA-MB-231 cells (10^5 cells/100 μl of PBS) *via* the left cardiac ventricle, as described previously (24, 25). On day 25, radiographs were obtained and hind limbs were processed, as described in the subsections below. The Animal Committee of Okayama University Graduate School of Medicine, Dentistry, and Pharmaceutical Sciences approved all of the experimental procedures.

Histochemistry and immunochemistry. Hind limb long bones of nude mice injected with cancer cells were excised, fixed in 10% neutral-buffered formalin, decalcified, and then embedded in paraffin. For immunochemistry, paraffin sections of mouse hind limb long bones were treated with 1500 units/ml bovine testis hyaluronidase in PBS containing 10% foetal bovine serum (FBS) for 3 h at 37˚C. They were then blocked with 10% goat serum and reacted with a 1:200 dilution of anti-VEGF, PTHrP or PTH1R antibodies overnight at 4˚C. Next, the sections were washed 3 times with PBS and thereafter reacted for 1 h with FITC or rhodamine-conjugated anti-rabbit or anti-mouse IgG serum in 3% BSA-PBS. The sections were finally washed 3 times with PBS, mounted, and viewed under a confocal microscope (BIO-RAD, Laboratories, Hercules, CA, USA).

Preparation of MDA-MB-231 conditioned medium. MDA-MB-231 cells (2×10^6) were seeded into a 10 cm diameter dish and cultured in 10% DMEM. After the cells had reached subconfluence, the medium was changed to serum-free DMEM with or without 100 nM PTHrP and incubated for 24 h. The vehicle- or PTHrP-treated MDA-MB-231 cells were centrifuged at 3000 rpm for 10 min, and the resulting clear supernatant was used as the conditioned medium for the assays described below.

[^{3}H] Thymidine incorporation assay. The proliferation of HUVECs was assessed by measuring the incorporation of [^{3}H] thymidine into the cells. HUVECs (1×10^4) were cultured in 96-well plates under the conditions described in the figure legends and were pulsed with 10 μCi/well of [^{3}H] thymidine (Amersham Biosciences, Buckinghamshire, UK) for 4 h during incubation

with test agents. The radioactivity incorporated into acid-precipitated material was counted by use of a microbeta scintillation counter (Micro Beta-PLUS; WALLAC, Pegasus Scientific Inc, Rockville, MD, USA).

Migration assay. Migration of HUVECs was studied by using Boyden chambers. HUVECs in logarithmic growth phase were detached by trypsin-EDTA, and 1×10^5 cells in endothelial medium without any supplements were added to polycarbonate membranes (pore size 8.0 mm; Becton Dickinson, Franklin Lakes, NJ, USA). 100 nM PTHrP- or vehicle-treated MDA-MB-231 culture medium with or without 100 nM PTHrP, 10 ng/ml VEGF or 25 g/ml VEGF-neutralising antibodies were added to the lower chamber, and the system was incubated at 37˚C for 8 h in 5% CO_2. After incubation and fixation, the non-migrating cells were removed with a cotton swab and the remaining cells were stained with 2% Crystal Violet (Sigma). The number of stained cells on the lower side of the membrane in 4 microscopic fields were counted, and the average of 3 wells was determined.

Rat aorta ring assay. Male Wistar rats (6 weeks old; Clea Japan, Inc, Tokyo, Japan) were housed, two to a metal cage, in a room with a controlled temperature (24±1˚C) and a 12 h light:dark cycle (lights on, 08:00-20:00 h). An *ex vivo* angiogenesis assay was performed according to the slightly modified method described elsewhere (26). Briefly, a male Wistar rat (body weight ~200 g) was sacrificed by bleeding from the right femoral artery under anaesthesia with diethyl ether. The thoracic aorta was removed and washed with RPMI-1640 medium to avoid contamination with blood. It was then turned inside out, and cut into segments of about 1-1.5 mm. Collagen gel (gel matrix solution) was made with 8 volumes of porcine tendon collagen solution (3 mg/ml) (Cellmatrix Ia, Nitta Gelatin Co, Osaka, Japan), 1 volume of 10×Eagle's MEM (Gibco, New York, USA), and 1 volume of reconstitution buffer (0.08 M NaOH and 200 mM HEPES). These solutions were mixed gently at 4˚C. Each aortic segment was placed in the center of a well on a 12-well culture plate and covered with 0.3 ml of gel matrix solution reconstituted as described above. The solution was allowed to gel at 37˚C for 20 min, and then overlaid with 0.8 ml of RPMI-1640 medium (Gibco) containing 1% ITS^+ (Becton Dickinson Labware, MA, USA). Test sample solution or vehicle was then added. Incubation was carried out for 5 days in a fully humidified system of 5% CO_2 in air at 37˚C. The medium was changed on day 1 and 3 of the culture period. An estimation of the length of the capillaries was made under phase-contrast microscopy by measuring the distance from the cut end of the aortic segment to the end of each capillary. Microscopic fields were photographed with a digital camera. The length and area of the capillaries were measured by using NIH Image (National Institute of Health, Bethesda, MD, USA). Each reported value is presented as the average of 3 culture samples.

Real-time RT-PCR. Total RNA was isolated from MDA-MB-231 cells by using TRIZOL reagent according to the manufacturer's recommendations. The transcripts encoded by $VEGF_{165}$ were amplified by RT-PCR using specific primers (27). The primers used were the following: 5'-CCCTGATGAGATCGAGTACATCTT-3' (forward) and 5'-AGCAAGGCCCACAGGGATTT-3' (reverse) for *VEGF*; and 5'-TGAACGGGAAGCTCACTGG-3' (forward) and 5'-TCCACCA CCCTGTTGCTGTA-3' (reverse) for *GAPDH*. Real-time RT-PCR was performed with a Light Cycler (Roche Molecular Biochemicals, Mannheim, Germany) in Light Cycler capillaries using a commercially available master mix containing Taq DNA polymerase and SYBR-Green I deoxyribonucleoside triphosphates (Light Cycler DNA master SYBR-Green I; Roche Molecular Biochemicals). After the addition of primers (final concentration: 10 μM), $MgCl_2$ (3 mM) and template DNA to the master mix, 65 cycles of denaturation (95˚C for 10s), annealing, (55˚C for 5s) and extension (72˚C for 10s) were performed. After the completion of PCR amplification, a melting curve analysis was performed.

Western blot analysis. Proteins were extracted from MDA-MB-231 cells and quantified by using a protein assay kit (BIO-RAD). Protein samples (20 μg) were fractionated by SDS-polyacrylamide gel (READYGELS, 10%; BIO-RAD) electrophoresis and transferred to polyvinylidene difluoride membranes (Immobilon-P, Millipore, Bedford MA, USA). Immunoblotting was carried out by using the antibodies indicated above. Bands were visualized by using the ECL chemiluminescence detection method (RPN 2109, Amersham Biosciences).

ELISA. The VEGF protein levels in the cell-conditioned medium were determined in triplicate by ELISA (Quantikine human VEGF immunoassay kit; R&D Systems). The sensitivity of the assay was less than 5.0 pg/ml.

DNA transfection and luciferase assay. For transient transfection studies, MDA-MB-231 cells were plated at a density of 1×10^5 cells per well in 12-well plates and incubated for 24 h in complete medium. The cells were then transfected with 0.5 μg of the siRNA constructs and 1 μg of the specific promoter-reporter constructs by using FuGENE 6 transfection reagent (Roche Basel, Switzland) following the manufacturer's instructions. A Renilla luciferase construct, phRL-TK(int-), was included as an internal control for transfection efficiency. All transfection experiments were repeated 3 times in duplicate.

Pit formation assay. $CD11b^+$ bone marrow cells were seeded on dentine slices that had been placed in 96-well plates (1 slice/well) (28) and were cultured for 5 days in αMEM containing RANKL (100 ng/ml) and M-CSF (30 ng/ml). The medium was then changed to conditioned medium from vehicle- or PTHrP-treated MDA-MB-231 cultures, and the cells were incubated for 48 h. Thereafter, the cells were removed from the dentine slices, and the resorbed area was stained with Mayer's hematoxylin. The area of pits on the slices was quantified by light microscopy and imaging analysis (BZ-8000, Keyence, Osaka, Japan). The results are expressed as the mean±SD of 3 cultures.

Statistical analysis. Data were analyzed by using an unpaired Student's *t*-test for analysis of the two groups, and Fisher's protected least significant difference (Fisher's PLSD) for analysis of multiple group comparisons. Results are expressed as the mean±S.D. $P<0.05$ was considered statistically significant.

Results

Co-localization of VEGF, PTHrP, and PTH1R in bone metastases. As VEGF levels are significantly elevated in regions of bone metastasis in patients (29), and PTHrP is the central mediator of osteolytic metastasis (30). The distribution patterns of VEGF, PTHrP, and PTH1R were first examined in regions of cancer metastasis to bone in

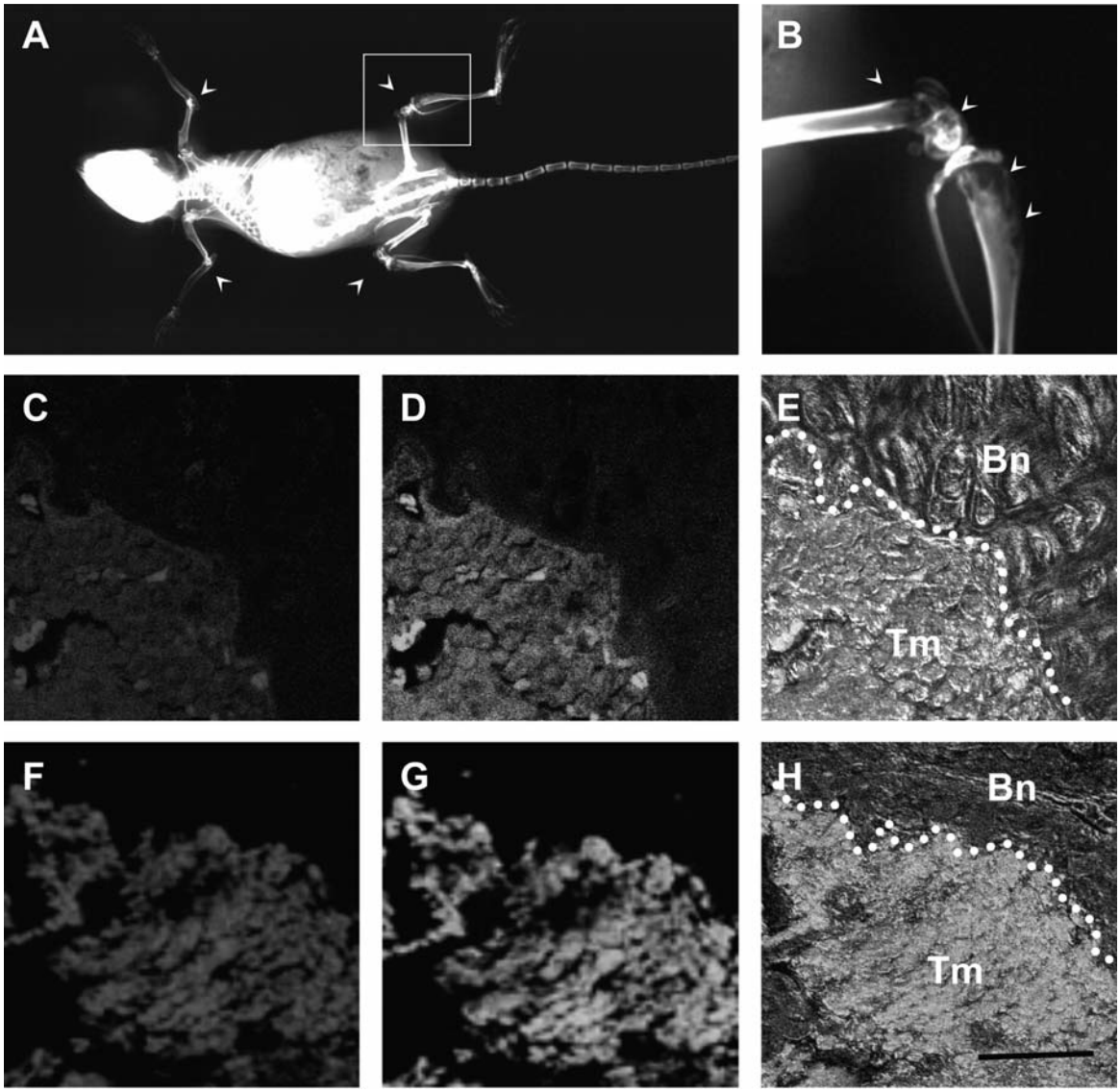

Figure 1. *A and B: Localization patterns of VEGF, PTH1R, and PTHrP in cancer cells showing osteolytic bone metastasis. Representative radiographs of hind limbs from mice 25 days after tumour inoculation. The arrowheads indicate osteolytic lesions. The area delimited by the square in 'A' is magnified in 'B'. C-F: Hind limbs from mice bearing MDA-MB-231 tumours were processed and analyzed by immunohistochemistry for the expression of VEGF (C), PTH1R (D and G) and PTHrP (F). E: The merged image of phase-contrast microscopic views 'C' and 'D'. H: The merged image of 'F' and 'G' with phase-contrast microscopic view of the same fields. Tm, Tumour cells; Bn, bone. Scale bar, 50 μm.*

mice. Radiography revealed various sites of osteolytic lesions (Figures 1A and B). VEGF (Figure 1C) and PTH1R (Figure 1D) were strongly expressed in cancer cells that had invaded into the bone matrix. PTHrP (Figure 1F) was also co-localized with PTH1R (Figure 1G) in the cancer cells (Figure 1H), supporting the idea that PTHrP may act in an autocrine manner on cancer cells in regions of bone metastasis. These results also indicate that PTHrP may regulate VEGF expression in cancer cells in the bone microenvironment.

PTHrP stimulates VEGF expression. Based on the above findings, cultured MDA-MB-231 cells were studied to determine whether PTHrP could regulate the expression of VEGF or not. Semi-confluent cultures were treated with increasing concentrations of PTHrP, and the resultant samples were processed for Western blot analysis. Incubation with PTHrP for 24 h significantly stimulated VEGF expression in dose-dependent manner (Figure 2A, lanes 3 and 4), whereas the expression of the housekeeping protein β-actin remained constant (Figure 2A). To verify

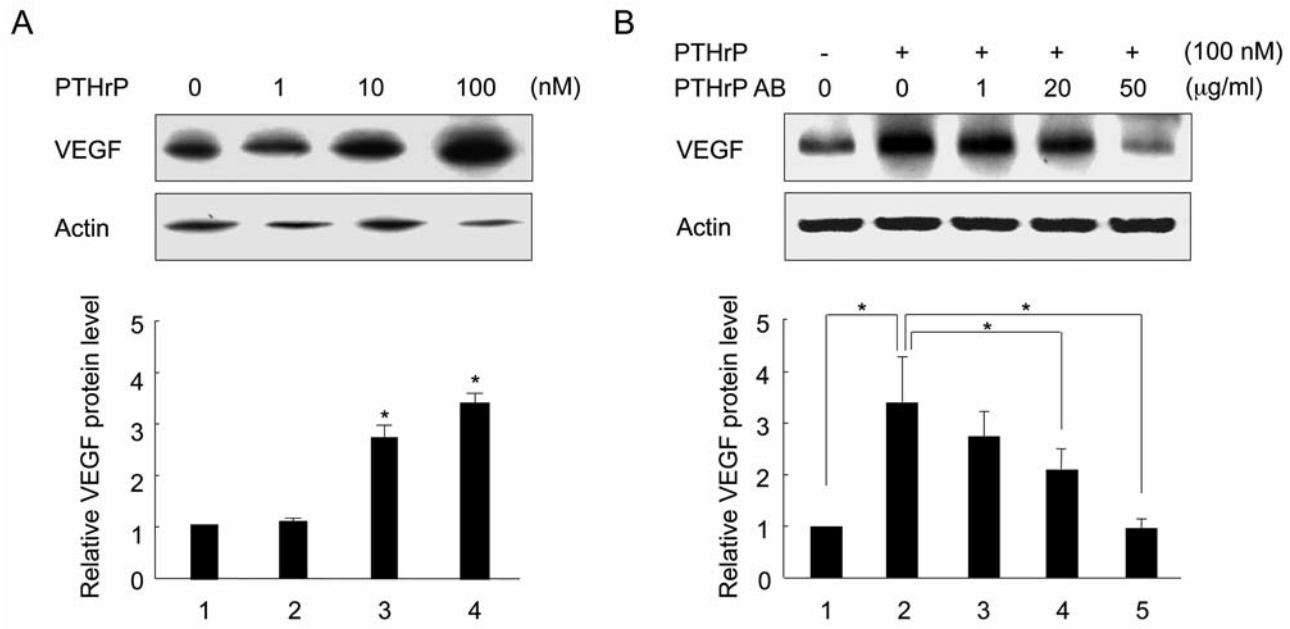

Figure 2. *Effect of PTHrP on the expression of VEGF in MDA-MB-231 cells. A, B: Immunoblot analysis of VEGF in MDA-MB-231 cells 24 h after treatment with the indicated amount of PTHrP in the presence or absence of PTHrP neutralizing antibody (PTHrP AB). Quantitative analysis by computer-assisted densitometry. Statistically-significant differences (*p<0.05) relative to controls (vehicle) are indicated by asterisks.*

the specificity of PTHrP action, MDA-MB-231 cells were incubated with 100 nM PTHrP for 24 h in the absence or presence of different concentrations of PTHrP-neutralizing antibody (1, 20 or 50 μg/ml). PTHrP boosted VEGF expression over the control value as expected (Figure 2B, *cf*. lanes 1 and 2), whereas increasing amounts of the neutralising antibody progressively reversed the PTHrP action, and 50 μg/ml antibody completely blocked it (Figure 2B, lane 5).

Effect of medium conditioned by PTHrP-stimulated MDA-MB-231 cells on the proliferation and migration of HUVECs and rat aorta ring endothelial cells. In order to confirm the angiogenic effect of PTHrP *in vitro*, HUVECs were treated with medium conditioned by vehicle-treated MDA-MB-231 cells (control-CM) or with that conditioned by 100 nM PTHrP-treated MDA-MB-231 cells (PTHrP-CM). The proliferation of HUVECs was stimulated more by PTHrP-CM than by control-CM and was significantly blocked by 50 μg/ml anti-VEGF antibodies added to either type of culture. In addition, 10 ng/ml VEGF stimulated the proliferation of control-CM-treated HUVECs, which was significantly blocked by 50 μg/ml anti-VEGF antibodies. However, treatment of control CM-treated HUVECs with 100 nM PTHrP failed to stimulate proliferation, and the proliferation was not changed by the addition of 50 μg/ml anti-VEGF antibody (Figure 3A).

Next the effect of PTHrP-CM on the migration of HUVECs was examined. Figure 3B shows that PTHrP-CM stimulated the migration of HUVECs more than did the control-CM treatment. Treatment with 50 μg/ml anti-VEGF antibody suppressed the PTHrP-CM-induced migration, and the inhibition was similar to the antibody-induced suppression of the VEGF-induced migration of control-CM-treated HUVECs. However, 100 nM PTHrP failed to stimulate migration of HUVECs in the control CM treatment group, and the proliferation was not affected by 50 μg/ml anti-VEGF antibody treatment (Figure 3B).

To further confirm the involvement of PTHrP in the VEGF production in MDA-MB-231 cells, the aorta ring assay was used (26). Inside-out rat aorta slices were maintained *in vitro* in control-CM to which had been added vehicle, 10 ng/ml VEGF, or 10 ng/ml VEGF+50 μg/ml anti-VEGF antibody, or in PTHrP-CM plus vehicle, 50 μg/ml control IgG, or 50 μg/ml anti-VEGF antibody. The additives were replaced every 2 days, and the angiogenic responses were evaluated on day 5. A few capillaries emerged from vehicle-treated rings in the control-CM (Figure 4A). However, the blood vessels were extended vigorously by the addition of VEGF, and their extension was inhibited by VEGF antibody. On the other hand, in the PTHrP-CM a large number of capillaries of fairly extended length (Figure 4B) and area (Figure 4C) were observed for both vehicle- and control IgG-treated rings (Figure 4A); and these responses were considerably suppressed by anti-VEGF antibody (Figure 4A-C).

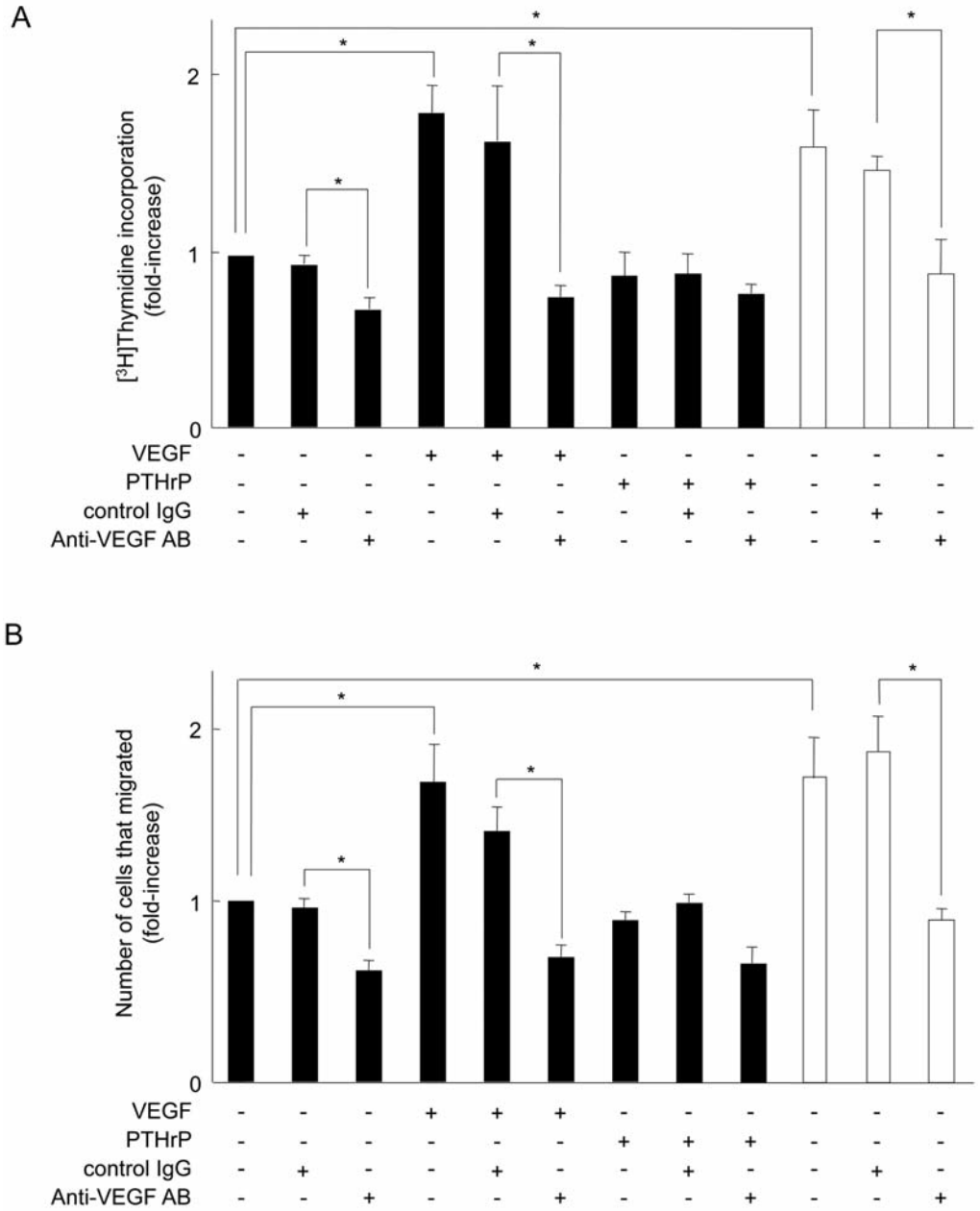

Figure 3. *Effect of conditioned medium from PTHrP-treated MDA-MB-231 cultures on the proliferation and migration of HUVECs. A: HUVECs were transferred to and kept in serum-reduced medium overnight and then incubated for 18 h in the presence of conditioned medium (serum-free) from vehicle- (solid column) or PTHrP- treated (open column) MDA-MB-231 cultures with or without 10 ng/ml VEGF, 100 nM PTHrP or 50 μg/ml anti-VEGF neutralizing antibodies. The [^{3}H] thymidine incorporation assay was performed as described in the Materials and Methods. B: Boyden chamber assay. Conditioned medium from vehicle (solid columns)- or PTHrP (open column)-stimulated MDA-MB-231 cultures with or without 10 ng/ml VEGF, 100 nM PTHrP or 50 μg/ml anti-VEGF antibodies was added to the lower chamber. Results are the means of independent experiments performed in triplicate. Asterisks indicate a significant difference at *$p<0.05$.*

Effect of PTHrP-CM on osteoclast formation. Next the effect of PTHrP-CM on the formation of osteoclasts was examined. PTHrP-CM increased the number of TRAP-positive CD11b$^+$ osteoclasts number more than did the control-CM, in which the number was similar to that obtained with 10 ng/ml VEGF in the control-CM. On the other hand, treatment with 50 μg/ml VEGF-neutralizing antibody inhibited both VEGF-induced osteoclast formation in control-CM and PTHrP-CM-induced osteoclast formation (Figure 5A). However, treatment with 100 nM PTHrP failed to stimulate osteoclast formation (data not shown).

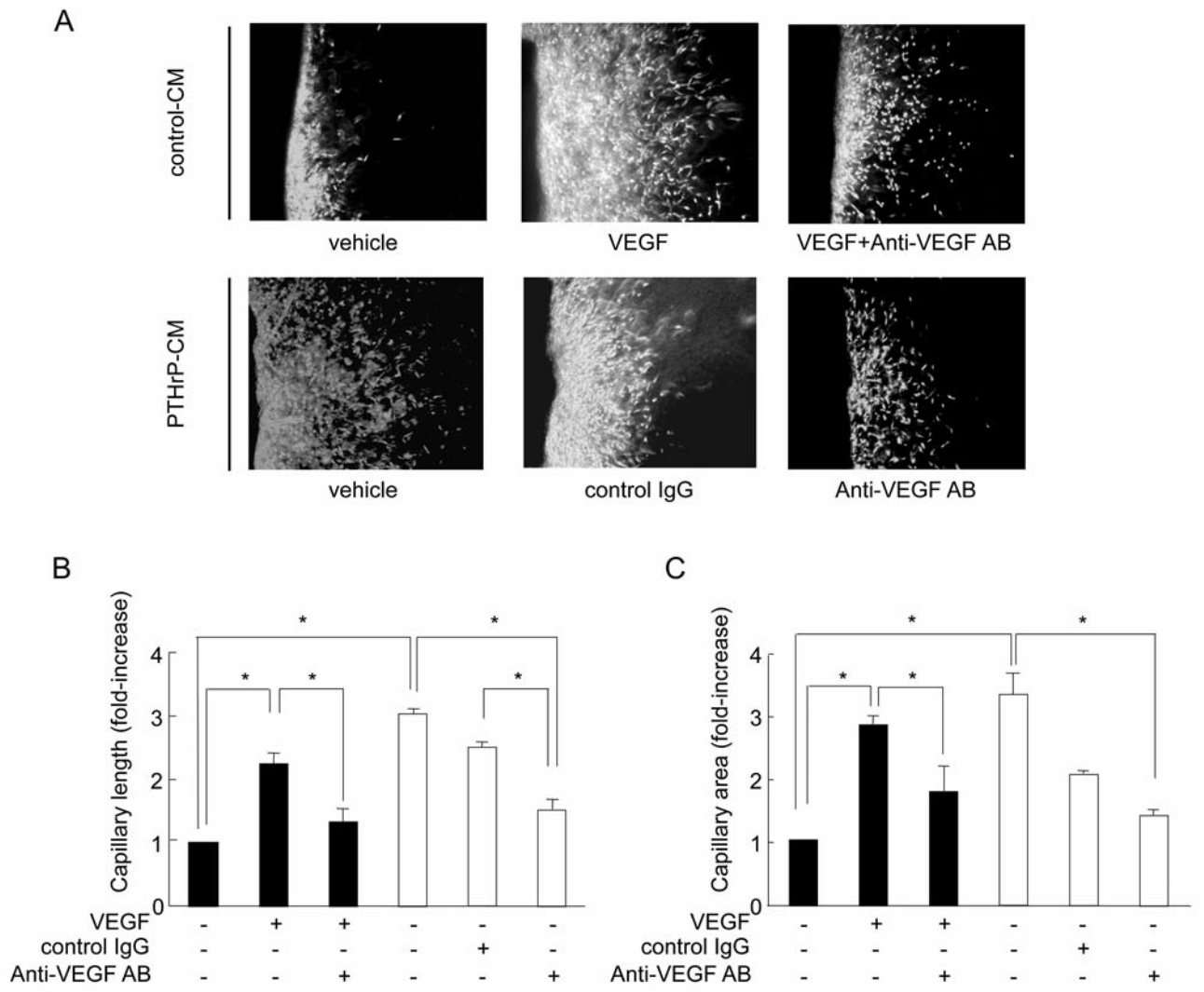

Figure 4. *Conditioned medium from PTHrP-treated MDA-MB-231 cultures stimulated the capillary growth of rat aortic segments cultured in collagen gel. Each aortic segment was isolated and cultured as described in the Materials and Methods. Aorta rings were observed on day 5 (A). The length (B) and area (C) of the capillaries were measured by using NIH Image. The data presented represent the results of a typical experiment, which was repeated more than 3 times with similar results. Solid columns: conditioned medium from vehicle-treated MDA-MB-231 cell cultures; open columns: conditioned medium from PTHrP-treated MDA-MB-231 cell cultures. Asterisks indicate significant difference at *p<0.05.*

PTHrP-CM stimulates osteoclasts to resorb a mineralized substrate. Next the area of resorption was examined by delineating the resorption pits and then processing these images with image analysis software. Pit formation of osteoclasts was stimulated more by PTHrP-CM than by control-CM, and in both cases was significantly blocked by 50 μg/ml VEGF antibody (Figures 5B and C). This confirmed that VEGF stimulated bone resorptive activity, and this stimulation was blocked by anti-VEGF antibody. However, treatment with 100 nM PTHrP failed to stimulate the resorption (data not shown).

PKA, PKC, and MAPK involvement in VEGF gene regulation by PTHrP. Based on the above findings and the fact that $VEGF_{165}$ is involved in tumour angiogenesis (31) and tumour-induced bone destruction (32), finally possible signaling pathways involved in the stimulation of $VEGF_{165}$ gene expression by PTHrP were examined. As shown in Figure 2, incubation of MDA-MB-231 cells with PTHrP for 24 h stimulated VEGF expression. To determine whether activation of PKA or PKC could mimic the effect of PTHrP on *VEGF* expression, semi-confluent cultures of MDA-MB-231 cells were treated with increasing amounts of db-cAMP, which

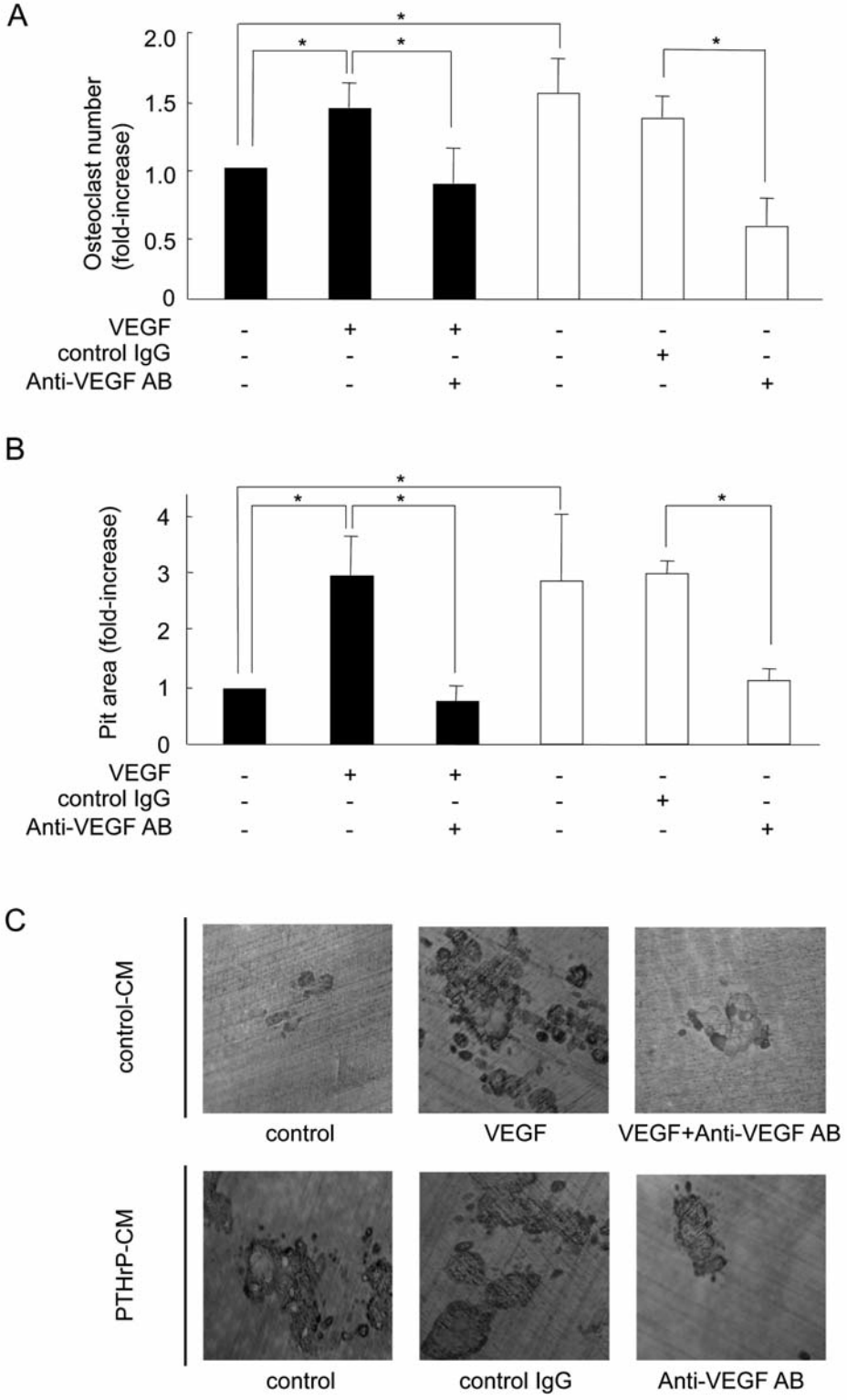

Figure 5. *Effect of conditioned medium from PTHrP-stimulated MDA-MB-231 cultures on osteoclast formation and pit formation. A: TRAP-positive multinucleate cells were counted manually under a light microscope. B and C: Pit formation assay. Cells treated as described in 'Pit formation assay' in the Materials and Methods were removed from dentine slices, and the resorbed areas were stained and quantified as described there. The pit area was measured by using NIH Image (B). Solid columns: conditioned medium from vehicle-treated MDA-MB-231 cultures; open columns: conditioned medium from PTHrP-treated MDA-MB-231 cultures. Asterisks indicate a significant difference at *p<0.05.*

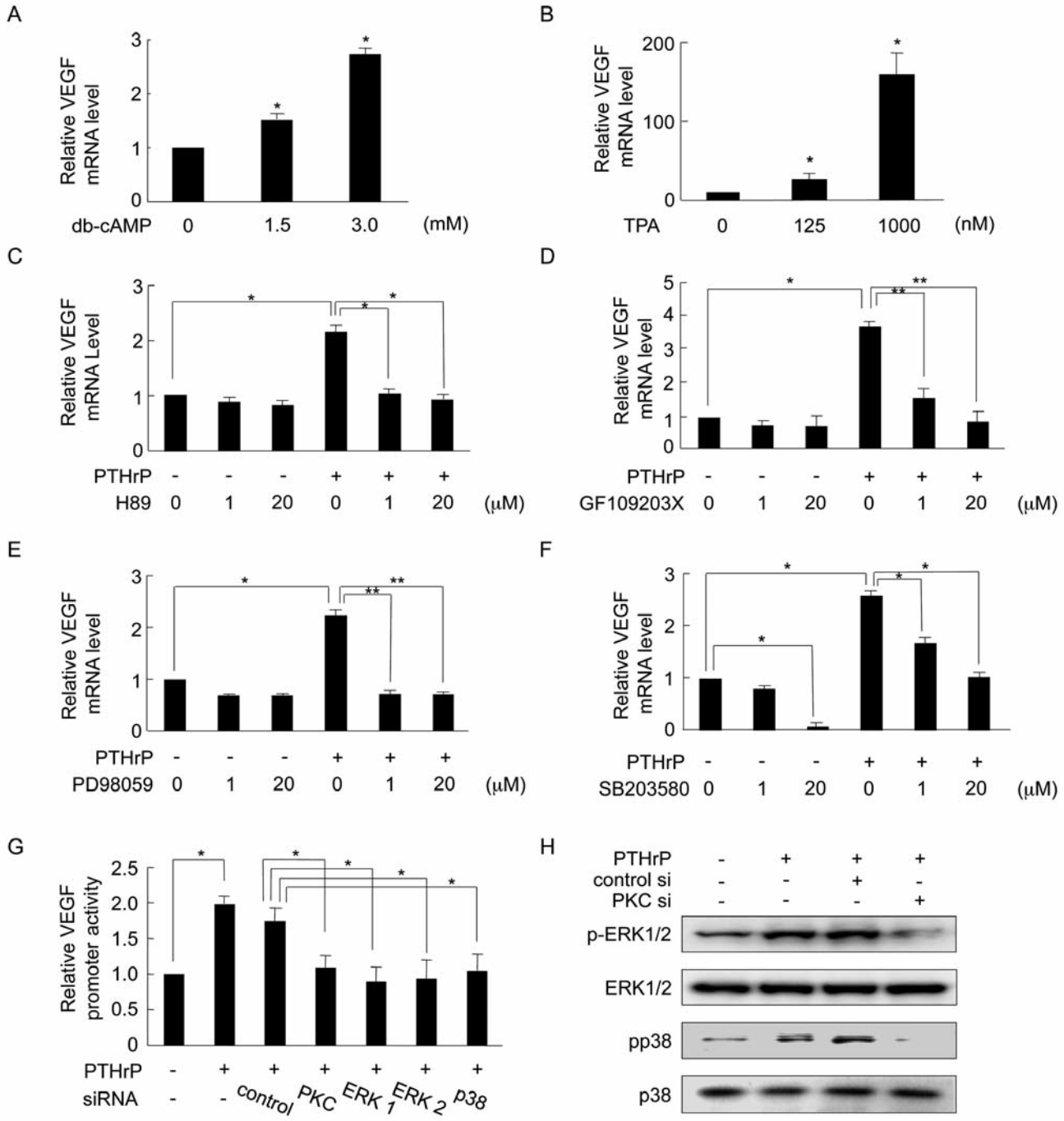

Figure 6. *Differential modulation of VEGF gene expression and promoter activity by PKA, PKC, and MAPK inhibitors. A, B: MDA-MB-231 cells were treated with the indicated doses of dibutyryl-cAMP (db-cAMP, A) or 12-O-tetradecanoylphorbol-13-acetate (TPA, B) for 8 h. C-F: MDA-MB-231 cells were preincubated with H89 (C), GF109203X (D), PD98059 (E) or SB203580 (F) for 30 min and then incubated with 100 nM PTHrP for 8 h. Total RNA was analysed by real-time RT-PCR (A-F). G: MDA-MB-231 cells were transiently transfected with a VEGF promoter-reporter construct with or without siRNAs for PKC, ERK1, ERK2 or p38, and then incubated or not with 100 nM PTHrP. After 24 h of incubation, firefly luciferase activity was measured. Values are shown as n-fold values relative to Renilla luciferase activity (internal control). H: The cells were transiently transfected with siRNA for PKC (PKC si) or with a control siRNA (control si), and then incubated with 100 nM PTHrP or not for 30 min. After stimulation, the cells were analyzed for p-ERK1/2, ERK1/2, p-p38 or p38 by Western blotting as described in the Materials and Methods. Mean values of the results of 3 experiments are displayed with error bars of SD. *p<0.05, Significantly different from control or as indicated by the brackets.*

activates PKA or of TPA, which activates PKC. Both treatments resulted in dose-dependent stimulation of *VEGF* expression (Figures 6A and B). Next, whether PKA and/or PKC mediated the effect of PTHrP on *VEGF* expression was examined by treating MDA-MB-231 cells with 100 nM PTHrP in the absence or presence of increasing amounts of H89 (a widely used inhibitor of PKA) or GF109203X (a widely used inhibitor of PKC). Treatment with H89 at 1 μM suppressed the PTHrP stimulation of *VEGF* expression (Figure 6C). GF109203X also significantly counteracted the PTHrP stimulation of *VEGF* expression dose dependently (Figure 6D). The possible roles of MAP kinases in *VEGF* induction were examined by PTHrP. MDA-MB-231 cells were exposed to 100 nM PTHrP for 8 h in the absence or presence of increasing concentrations of PD98059 (a widely used inhibitor of MEK1/2 kinases) or SB203580 (a widely used inhibitor of p38 kinase). Treatment with PD98059 or SB203580 completely neutralised the PTHrP-induced stimulation of *VEGF* expression (Figures 7E and F). However, increasing amounts of or SP600125 (a widely used inhibitor of JNK) failed to suppress the PTHrP-stimulated *VEGF* expression (data not shown).

Effect of PTHrP on transcriptional activity of VEGF proximal promoter. Because real-time RT-PCR analysis suggested that PTHrP up-regulation of *VEGF* expression was dependent on PKA, PKC, ERK1/2, and p38 MAPK pathways, a *VEGF* promoter reporter construct was employed to analyze the regulatory mechanism of *VEGF* induction by PTHrP. The activity of the 1.9-kb VEGF promoter construct was induced by PTHrP, and was decreased by pretransfection with siRNAs against PKC, pERK1, pERK2, or p38 (Figure 6G).

Effect of PTHrP on the activation of ERK1/2 and p38 MAPK activities. Finally the involvement of ERK1/2 and p38 MAPK in PTHrP action was analysed. PTHrP treatment resulted in increased levels of phosphorylated ERK1/2 and p38 MAPK, as revealed by Western blot analysis, whereas overall ERK1/2 and p38 levels remained unchanged. Subsequently, to examine the relationship phosphorylation of the MAPKs and PKC, cells were transfected with siPKC and then treated with 100 nM PTHrP. As a result, both ERK1/2 and p38 activation by PTHrP were blocked by the down-regulation of PKC, whereas control si-pretreated cells showed the presence of p-ERK1/2 and p-p38 MAPK (Figure 6H).

Discussion

Previous studies have implicated PTHrP as a common osteolytic factor and VEGF as a major player in the pathogenesis of breast cancer (33). In the present study, a bone metastatic model was developed that may explain the interrelationship between these molecules and account for the high osteolysis due to breast cancer metastasis. The major findings of this study are the following: (i) VEGF production was mediated by PTHrP and controlled by an autocrine loop in which PTHrP engages PTH1R. (ii) PTHrP-induced VEGF expression supported HUVEC proliferation and migration. (iii) PTHrP-induced VEGF expression up-regulated osteoclast formation and pit formation.

In the bone microenvironment, the existence of multiple sources of both VEGF and other tumour-produced cytokines creates a complex scenario for the regulation of osteoclasts. The direct *in vivo* action of VEGF on osteoclasts in developing mouse bone, similar to these *in vitro* findings, is clearly supported by the dramatic inhibitory effect on osteoclasts/chondroclasts elicited by blocking VEGF with soluble Flt-1 (13). Flt1 tyrosine kinase domain gene $(TK)^{-/-}$ mice showed a much lower number of osteoclasts than did $Flt1TK^{+/+}$ mice (34, 35). The present findings suggest that Flt-1 sequestration of VEGF should also diminish Flt-1 signaling in osteoclast precursors and osteoclasts, rather than exclusively acting on endothelial cell targets. This could explain the observed physiological and pathological linkage between osteoclastic resorption and endothelial cell proliferation and migration.

Conditioned medium obtained from tumour cells is known to induce bone resorption *in vitro* (36) . However, the soluble factors that activate osteoclasts have not yet been fully elucidated. One candidate is PTHrP, which was originally identified as a hypercalcaemic factor in MDA-MB-231 breast cancer cells (37). PTHrP activates osteoclastic bone resorption through binding to the PTH1R on osteoblasts and increasing the expression of RANKL on osteoblasts (38). Transforming growth factor beta (TGF-β) released from bone matrix during osteolysis is believed to stimulate tumour cells to produce more PTHrP, which in turn activates osteoclasts (1). Tumour cells may also up-regulate PTH1R expression as a result of their exposure to the bone microenvironment. Such action may be realized by growth factors present in the bone marrow, which factors stimulate the production of endogenous PTHrP by cancer cells. VEGF expression was specifically observed in PTH1R-positive cancer cells that had invaded the bone marrow. Therefore, the observed osteolytic property may include an autocrine action to yield increased VEGF expression in response to PTHrP. This vicious cycle of tumour cell–bone microenvironment interaction results in bone destruction and tumour growth. These findings together indicate that the large amount of PTHrP and PTH1R, as well as the VEGF secreted by MDA-MB-231 cells, may be the main reason for their high bone metastatic activity.

This study provides an insight into the mechanism by which PTHrP induces *VEGF* mRNA expression in MDA231 cells. Exogenous PTHrP stimulation of the cells with exogenous PTHrP induced the phosphorylation of ERK and p38 MAPK. PTHrP-induced *VEGF* expression in MDA-MB-231 cells occurred in an ERK- and p38 MAPK-

dependent manner. These results are consistent with previous studies, which show that PTHrP stimulates ERK and p38 MAPK activation in osteogenic cells, osteosarcoma cells and calvarial osteoblasts (19, 39, 40), and MDA-MB-231 cells (25). Both PKA and PKC have been reported to regulate the ERK and p38 MAPK pathway as well, and the effects seems to be highly cell-type specific (41). In this study, it was shown that the PKC pathway signals also stimulated ERK and p38 MAPK activity in MDA-MB-231 cells. A possible biological significance of this phenomenon may be that the cooperative activation of ERK and p38 MAPK by PTHrP may be required for the induction of *VEGF* to yield a profound consequence of tumour growth and survival in regions of bone metastasis. These data taken together suggest that the net stimulation of *VEGF* expression ought to be the result of the ERK and p38 MAPK-mediated strong induction in those breast cancer cells. It should be also noted that p38 MAPK mediates the TGF-β-stimulated PTHrP production in MDA-MB-231 cells (30). Thus, in the co-presence of TGF-β, even p38 MAPK can be considered to be an indirect mediator of *VEGF* induction (42).

Finally, to determine the target of the MAPK-transduced PTHrP signal for *VEGF* expression, we examined the effects of PTHrP on the *VEGF* proximal promoter in the kinase siRNA study. The results of the *VEGF* promoter assay suggest that this regulation was effected at the transcriptional level. Moreover, blockade of ERK1/2, p38, and PKC partially decreased the basal and PTHrP-induced activity of the *VEGF* promoter. These data indicate that PKC-ERK1/2 and PKC-p38 pathways may play a role in the regulation of *VEGF* promoter activity. At present, it is difficult to define completely the mechanisms of the regulation in the PTHrP-induced activation of the *VEGF* promoter. However it is possible that the transcription factor Sp1 is activated by ERK and induces VEGF production in other cells. Yin *et al*. demonstrated that the AP-1 pathway is involved in VEGF expression in breast cancer cells (43). The transcription factor AP-1, as do other components in the AP-1 complex, serve as substrates for MAPK, and an AP-1 binding site exists in the promoter region of the *VEGF* gene (44). Additionally, a some studies have found that MAPK regulation by PKA requires STAT3 in breast cancer cells (45). These transcription factors, downstream of the PTHrP signaling cascade, might involved in the induction of *VEGF* transcription in MDA-MB-231 cells.

In this study it was shown that PTHrPR, PTHrP, and VEGF are expressed in breast cancer cells and thus may mediate autocrine PTHrP signaling to stimulate the production of VEGF in the bone microenvironment. PTHrP induced PKC, ERK MAPK, and p38 MAPK pathways, ultimately resulting in VEGF expression. The elucidation of this regulation may have strong implications for our understanding of the multifunctional roles played by VEGF in the relationship between bone/cartilage resorption and angiogenesis.

Acknowledgements

We thank Drs Hiroshi Nakagawa, Masahiro Iwamoto and Maurizio Pacifici for useful advice and Dr Daniel Chung for human VEGF promoter luciferase constructs. This work was supported in part by grants from the Okayama Health Foundation (to TS), the Ryobi-teien Memorial Foundation (to TS), and the programs Grants-in-Aid for Young Scientists (A) [to TS] and Scientific Research (B) [to AS] from the Ministry of Education, Culture, Sports, Science and Technology of Japan.

References

1 Liao J and McCauley LK: Skeletal metastasis: Established and emerging roles of parathyroid hormone related protein (PTHrP). Cancer Metastasis Rev *25*: 559-571, 2006.
2 Yoneda T and Hiraga T: Crosstalk between cancer cells and bone microenvironment in bone metastasis. Biochem Biophys Res Commun *328*: 679-687, 2005.
3 Henderson MA, Danks JA, Slavin JL, Byrnes GB, Choong PF, Spillane JB, Hopper JL and Martin TJ: Parathyroid hormone-related protein localization in breast cancers predict improved prognosis. Cancer Res *66*: 2250-2256, 2006.
4 Roodman GD: Mechanisms of bone metastasis. N Engl J Med *350*: 1655-1664, 2004.
5 DaSilva J, Gioeli D, Weber MJ and Parsons SJ: The neuroendocrine-derived peptide parathyroid hormone-related protein promotes prostate cancer cell growth by stabilizing the androgen receptor. Cancer Res *69*: 7402-7411, 2009.
6 Shen X and Falzon M: PTH-related protein up-regulates integrin alpha6beta4 expression and activates Akt in breast cancer cells. Exp Cell Res *312*: 3822-3834, 2006.
7 Nishihara M, Kanematsu T, Taguchi T and Razzaque MS: PTHrP and tumorigenesis: is there a role in prognosis? Ann N Y Acad Sci *1117*: 385-392, 2007.
8 Saito H, Tsunenari T, Onuma E, Sato K, Ogata E and Yamada-Okabe H: Humanized monoclonal antibody against parathyroid hormone-related protein suppresses osteolytic bone metastasis of human breast cancer cells derived from MDA-MB-231. Anticancer Res. *25*: 3817-3823, 2005.
9 Ferrara N: Vascular endothelial growth factor and the regulation of angiogenesis. Recent Prog Horm Res *55*: 15-35, 2000.
10 Shibuya M: Differential roles of vascular endothelial growth factor receptor-1 and receptor-2 in angiogenesis. J Biochem Mol Biol *39*: 469-478, 2006.
11 Purpura KA, George SH, Dang SM, Choi K, Nagy A and Zandstra PW: Soluble Flt-1 regulates Flk-1 activation to control hematopoietic and endothelial development in an oxygen-responsive manner. Stem Cells *26*: 2832-2842, 2008.
12 Usui T, Ishida S, Yamashiro K, Kaji Y, Poulaki V, Moore J, Moore T, Amano S, Horikawa Y, Dartt D, Golding M, Shima DT and Adamis AP: VEGF164(165) as the pathological isoform: differential leukocyte and endothelial responses through VEGFR1 and VEGFR2. Invest Ophthalmol Vis Sci *45*: 368-374, 2004.

13 Gerber HP, Vu TH, Ryan AM, Kowalski J, Werb Z and Ferrara N: VEGF couples hypertrophic cartilage remodeling, ossification and angiogenesis during endochondral bone formation. Nat Med *5:* 623-628, 1999.

14 Aldridge SE, Lennard TW, Williams JR and Birch MA: Vascular endothelial growth factor receptors in osteoclast differentiation and function. Biochem Biophys Res Commun *335*: 793-798, 2005.

15 Nakagawa M, Kaneda T, Arakawa T, Morita S, Sato T, Yomada T, Hanada K, Kumegawa M and Hakeda Y: Vascular endothelial growth factor (VEGF) directly enhances osteoclastic bone resorption and survival of mature osteoclasts. FEBS Lett *473*: 161-164, 2000.

16 Yang Q, McHugh KP, Patntirapong S, Gu X, Wunderlich L and Hauschka PV: VEGF enhancement of osteoclast survival and bone resorption involves VEGF receptor-2 signaling and beta3-integrin. Matrix Biol *27*: 589-599, 2008.

17 Esbrit P, Alvarez-Arroyo MV, De Miguel F, Martin O, Martinez ME and Caramelo C: *C*-Terminal parathyroid hormone-related protein increases vascular endothelial growth factor in human osteoblastic cells. J Am Soc Nephrol *11*: 1085-1092, 2000.

18 de Gortazar AR, Alonso V, Alvarez-Arroyo MV and Esbrit P: Transient exposure to PTHrP (107-139) exerts anabolic effects through vascular endothelial growth factor receptor 2 in human osteoblastic cells *in vitro*. Calcif Tissue Int. *79*: 360-369, 2006.

19 Alonso V, de Gortázar AR, Ardura JA, Andrade-Zapata I, Alvarez-Arroyo MV and Esbrit P: Parathyroid hormone-related protein (107-139) increases human osteoblastic cell survival by activation of vascular endothelial growth factor receptor-2. J Cell Physiol *217*: 717-727, 2008.

20 Ardura JA, Berruguete R, Rámila D, Alvarez-Arroyo MV and Esbrit P: Parathyroid hormone-related protein interacts with vascular endothelial growth factor to promote fibrogenesis in the obstructed mouse kidney. Am J Physiol Renal Physiol *295*: 415-425, 2008.

21 Onuma E, Sato K, Saito H, Tsunenari T, Ishii K, Esaki K, Yabuta N, Wakahara Y, Yamada-Okabe H and Ogata E: Generation of a humanized monoclonal antibody against human parathyroid hormone-related protein and its efficacy against humoral hypercalcemia of malignancy. Anticancer Res *24*: 2665-2673, 2004.

22 Mizukami Y, Li J, Zhang X, Zimmer MA, Iliopoulos O and Chung DC: Hypoxia-inducible factor-1-independent regulation of vascular endothelial growth factor by hypoxia in colon cancer. Cancer Res *1*: 1765-1772, 2004.

23 Cailleau R, Young R, Olive M and Reeves WJ Jr: Breast tumor cell lines from pleural effusions. J Natl Cancer Inst *53*: 661-674, 1974.

24 Sasaki A, Boyce BF, Story B, Wright KR, Chapman M, Boyce R, Mundy GR and Yoneda T: Bisphosphonate risedronate reduces metastatic human breast cancer burden in bone in nude mice. Cancer Res *55*: 3551-3557, 1995.

25 Shimo T, Kubota S, Yoshioka N, Ibaragi S, Isowa S, Eguchi T, Sasaki A and Takigawa M: Pathogenic role of connective tissue growth factor (CTGF/CCN2) in osteolytic metastasis of breast cancer. J Bone Miner Res *21*: 1045-1059, 2006.

26 Matsubara K, Mori M and Mizushina Y: Petasiphenol which inhibits DNA polymerase lambda activity is an inhibitor of *in vitro* angiogenesis. Oncol Rep *11*: 447-451, 2004.

27 Wellmann S, Taube T, Paal K, Graf V Einsiedel H, Geilen W, Seifert G, Eckert C, Henze G and Seeger K: Specific reverse transcription-PCR quantification of vascular endothelial growth factor (VEGF) splice variants by LightCycler technology. Clin Chem *47*: 654-660, 2001.

28 Jacquin C, Gran DE, Lee SK, Lorenzo JA and Aguila HL: Identification of multiple osteoclast precursor populations in murine bone marrow. J Bone Miner Res *21*: 67-77, 2006.

29 Wu D, Zhau HE, Huang WC, Iqbal S, Habib FK, Sartor O, Cvitanovic L, Marshall FF, Xu Z and Chung LW: cAMP-responsive element-binding protein regulates vascular endothelial growth factor expression: implication in human prostate cancer bone metastasis. Oncogene *26*: 5070-5077, 2007.

30 Kakonen SM, Selander KS, Chirgwin JM, Yin JJ, Burns S, Rankin WA, Grubbs BG, Dallas M, Cui Y and Guise TA: Transforming growth factor-beta stimulates parathyroid hormone-related protein and osteolytic metastases *via* Smad and mitogen-activated protein kinase signaling pathways. J Biol Chem *277*: 24571-24578, 2002.

31 Applanat MP, Buteau-Lozano H, Herve MA and Corpet A: Vascular endothelial growth factor is a target gene for estrogen receptor and contributes to breast cancer progression. Adv Exp Med Biol *617*: 437-444, 2008.

32 Guan H, Zhou Z, Wang H, Jia SF, Liu W and Kleinerman ES: A small interfering RNA targeting vascular endothelial growth factor inhibits Ewing's sarcoma growth in a xenograft mouse model. Clin Cancer Res *11*: 2662-2669, 2005.

33 Matsui J, Funahashi Y, Uenaka T, Watanabe T, Tsuruoka A and Asada M: Multi-kinase inhibitor E7080 suppresses lymph node and lung metastases of human mammary breast tumor MDA-MB-231 *via* inhibition of vascular endothelial growth factor-receptor (VEGF-R) 2 and VEGF-R3 kinase. Clin Cancer Res *14*: 5459-5465, 2008.

34 Niida S, Kondo T, Hiratsuka S, Hayashi S, Amizuka N, Noda T, Ikeda K and Shibuya M: VEGF receptor 1 signaling is essential for osteoclast development and bone marrow formation in colony-stimulating factor 1-deficient mice. Proc Natl Acad Sci USA. *102*: 14016-14021, 2005.

35 Otomo H, Sakai A, Uchida S, Tanaka S, Watanuki M, Moriwaki S, Niida S and Nakamura T: Flt-1 tyrosine kinase-deficient homozygous mice result in decreased trabecular bone volume with reduced osteogenic potential. Bone *40*: 1494-1501, 2007.

36 Tada T, Shin M, Fukushima H, Okabe K, Ozeki S, Okamoto M and Jimi E: Oral squamous cell carcinoma cells modulate osteoclast function by RANKL-dependent and -independent mechanisms. Cancer Lett *274*: 126-131, 2009.

37 Clines GA and Guise TA: Hypercalcaemia of malignancy and basic research on mechanisms responsible for osteolytic and osteoblastic metastasis to bone. Endocr Relat Cancer *12*: 549-583, 2005.

38 Akhtari M, Mansuri J, Newman KA, Guise TM and Seth P: Biology of breast cancer bone metastasis. Cancer Biol Ther *7*: 3-9, 2008.

39 Swarthout JT, Doggett TA, Lemker JL and Partridge NC: Stimulation of extracellular signal-regulated kinases and proliferation in rat osteoblastic cells by parathyroid hormone is protein kinase C-dependent. J Biol Chem *276*: 7586-7592, 2001.

40 Chen C, Koh AJ, Datta NS, Zhang J, Keller ET, Xiao G, Franceschi RT, D'Silva NJ and McCauley LK: Impact of the mitogen-activated protein kinase pathway on parathyroid hormone-related protein actions in osteoblasts. J Biol Chem *279*: 29121-29129, 2004.

41 Sriraman V, Modi SR, Bodenburg Y, Denner LA and Urban RJ: Identification of ERK and JNK as signaling mediators on protein kinase C activation in cultured granulosa cells. Mol Cell Endocrinol *294*: 52-60, 2008.
42 Wang L, Kwak JH, Kim SI, He Y and Choi ME: Transforming growth factor-beta1 stimulates vascular endothelial growth factor 164 *via* mitogen-activated protein kinase kinase 3-p38alpha and p38delta mitogen-activated protein kinase-dependent pathway in murine mesangial cells. J Biol Chem *279*: 33213-33219, 2004.
43 Yin Y, Wang S, Sun Y, Matt Y, Colburn NH, Shu Y and Han X: JNK/AP-1 pathway is involved in tumor necrosis factor-alpha induced expression of vascular endothelial growth factor in MCF7 cells. Biomed Pharmacother *63*: 429-435, 2009.
44 Chang HJ, Park JS, Kim MH, Hong MH, Kim KM, Kim SM, Shin BA, Ahn BW and Jung YD: Extracellular signal-regulated kinases and AP-1 mediate the up-regulation of vascular endothelial growth factor by PDGF in human vascular smooth muscle cells. Int J Oncol *28*: 135-141, 2006.
45 Xu H, Washington S, Verderame MF and Manni A: Activation of protein kinase A (PKA) signaling mitigates the antiproliferative and antiinvasive effects of alpha-difluoromethylornithine in breast cancer cells. Breast Cancer Res Treat *107*: 63-70, 2008.

Received March 31, 2010
Revised May 14, 2010
Accepted May 18, 2010